Solid-State Compaction and Drawing of Nascent Reactor Powders of Ultra-High-Molecular-Weight Polyethylene

Yong Lak Joo,[1] Huajun Zhou,[1] Seung-Goo Lee,[2] Hwan-Koo Lee,[3] Jae Kyung Song[3]

[1]*School of Chemical and Biomolecular Engineering, Cornell University, Ithaca, New York 14853*
[2]*Department of Textile Engineering, Chungnam National University, Yusung-gu, Daejeon 305-764, Korea*
[3]*Hanwha Chemical Research Center, 6 Shinsung-dong, Yusung-ku, Daejeon 305-345, Korea*

Received 15 August 2004; accepted 6 February 2005
DOI 10.1002/app.22076
Published online in Wiley InterScience (www.interscience.wiley.com).

ABSTRACT: The continuous production of ultra-high-molecular-weight polyethylene (UHMWPE) filaments was studied by the direct roll forming of nascent reactor powders followed by subsequent multistage orientation drawing below their melting points. The UHMWPE reactor powders used in this study were prepared by the polymerization of ethylene in the presence of soluble magnesium complexes, and they exhibited high yield even at low reaction temperatures. The unique, microporous powder morphology contributed to the successful compaction of the UHMWPE powders into coherent tapes below their melting temperatures. The small-angle X-ray scattering study of the compacted tapes revealed that folded-chain crystals with a relatively long-range order were formed during the compaction and were transformed into extended-chain crystals as the draw ratio increased. Our results also reveal that the drawability and tensile and thermal properties of the filaments depended sensitively on both the polymerization and solid-state processing conditions. The fiber drawn to a total draw ratio of 90 in the study had a tensile strength of 2.5 GPa and a tensile modulus of 130 GPa. Finally, the solid-state drawn UHMWPE filaments were treated with O_2 plasma, and the enhancement of the interfacial shear strength by the surface treatment is presented. © 2005 Wiley Periodicals, Inc. J Appl Polym Sci 98: 718–730, 2005

Key words: drawing; fibers; polyethylene (PE); strength; surfaces

INTRODUCTION

There has long been a growing interest in the development of solvent-free routes to high-modulus, high-strength polyethylene (PE) products.[1–3] Most solvent-free processes use as-polymerized or nascent, crystallizable ultra-high-molecular-weight polyethylene (UHMWPE).[4–9] It has been recognized that under certain experimental conditions, monomers may simultaneously polymerize and crystallize into a nonentangled conformation. UHMWPE films have been produced by the deposition of a vanadium catalyst system on glass slides followed by the polymerization of ethylene at relatively low temperatures.[4–6] Another route is the use of powder processing. Nascent UHMWPE reactor powders synthesized at low temperature in the presence of SiO_2-supported vanadium catalyst system are compacted and drawn.[7] These methods, however, lack industrial significance because either the yield of polymerization is not high enough or a continuous production method cannot be employed. Kanamoto et al. developed a two-stage drawing process for reactor powders, and tensile moduli over 100 GPa were obtained.[10] Nippon Oil Co. developed several solid-state processing routes for making strong and stiff PE tapes. Their process consisted of three stages: compaction, roll drawing, and tensile drawing had advanced to pilot plant stage.[11,12] Although the products obtained from the three-stage scheme possessed tensile moduli up to 120 GPa and moderate tensile strengths up to 1.9 GPa, the polymerization yield was still low.

This study refined this attractive route to high-performance PE filaments that does not require melting or dissolution before drawing. The major improvements of this solid-state process were based on both effective polymerization and simple deformation processes. The effective synthesis of nascent UHMWPE powders was achieved by the polymerization of ethylene in the presence of soluble magnesium complexes.[13,14] This polymerization was characterized by a high yield of UHMWPE even at low temperatures and directly produced polymers in an untangled conformation.[14] Such as-polymerized PE without further treatment could readily be compacted below its melting point and drawn into high-strength films or filaments.[15] This straightforward continuous process, which is composed of the roll compaction and subsequent tensile drawing of the filaments below their melting points, was investigated in this study.

Correspondence to: Y. L. Joo (ylj2@cornell.edu).

The purpose of this article is twofold. First, the molecular structures and thermal properties of the UHMWPE tapes directly formed by rolling below melting points of the powders are examined. The UHMWPE reactor powders were synthesized at various temperatures and pressures, and the effect of the polymerization conditions on the structures and thermal properties of the UHMWPE tapes were studied. The continuous production of the compacted tapes is essential in the continuous production of high-modulus, high-strength PE fibers. We adopted a direct roll-forming process, which is the most effective way to prepare monolithic materials from powders. This method is widely used for the processing of powdered metals, ceramics, and other materials.[3] In the direct roll-forming process, the capture of powders by the surfaces of two rolls provides a continuous feeding of the material into a narrowed clearance between the rolls where big normal and tangential stresses are created. Rolling is performed at a temperature lower than melting temperature of the reactor powder. For this monolithic materials preparation to be successful, however, the control of the powder morphology is important. Later, we demonstrate that the soluble magnesium complex catalyst system provided a unique, microporous powder morphology, which resulted in successful compaction of the UHMWPE powders into coherent tapes at low temperatures. We demonstrate that folded-chain crystals with a relatively long range order were formed during the compaction.

After examining the structure and thermal properties of the compacted UHMWPE tapes, we turn to the second segment of this article, in which the effects of the key parameters in the solid-state drawing on the thermal and tensile properties of the drawn tapes are presented. The strip cut width of the tapes, the deformation rate, and the temperature were varied in the drawing process, and the thermal behavior and tensile properties of the drawn tapes were measured at increasing draw ratios. The effects of the polymerization conditions on the thermal and tensile properties of the drawn tapes were also investigated. It is shown that the thermal behavior and tensile properties of the drawn tapes depended sensitively on the polymerization conditions and the solid-state processing conditions. Finally, solid-state drawn UHMWPE filaments were treated with O_2 plasma, and the enhancement of the interfacial shear strength by the surface treatment is presented.

EXPERIMENTAL

UHMWPE synthesis[13,14]

The UHMWPE used in this study was prepared by the polymerization of ethylene in an inert hydrocarbon solvent in the presence of a catalyst system composed of (1) titanium tetrachloride, (2) aluminum–organic compound, (3) tetrahydrofuran, and (4) soluble magnesium–organic compound prepared by the reaction of metal magnesium with chlorobutane in the presence of triethylaluminum. Polymerization was conducted for 1 h at five different polymerization temperatures (10–90°C) and two ethylene pressures (15 and 40 psia).

Characterization

Molecular weight

The molecular weight of each powder was estimated from its intrinsic viscosity [viscosity-average molecular weight (M_v)] in decalin at 135°C measured by an automatic viscometer (Cannon AUTOVISC I, State College, PA); the three polymer concentrations applied were 0.05, 0.1, and 0.15 g/L. The intrinsic viscosities of all of the samples were in the range 6–25 dL/g, which corresponded to average molecular weights of $0.5–4 \times 10^6$.

Thermal properties

Each sample was set in a DSC apparatus (DuPont 2100, Newtown, CT). The melting peak temperature and heat of fusion of each sample were measured at a heating rate of 10°C/min. After the first run, each sample was cooled, and a scan was carried out at the same heating rate to determine the differences in both melting temperature and heat of fusion between the two subsequent melting runs.

Powder characterization

The pore volume and specific inner surface area for the UHMWPE reactor powders were determined with a mercury intrusion porosimeter (Porosimeter 2000, Fisons Instruments, Beverly, MA). The particle morphologies of various UHMWPE powders was directly examined by scanning electron microscopy (SEM) to assess the micropore structures of the powders.

X-ray diffraction

X-ray diffraction measurements were done on a diffractometer with nickel-filtered Cu Kα radiation (wavelength = 0.15406 nm) operating at 45 kV and 100 mA. The diffractometer was equipped with Soller slits in both the incident and reflected beams. Data were collected in the 2θ range 15–40° in steps of 0.04° and at a scanning rate of 4 s/point. In small-angle X-ray scattering (SAXS) experiments, data were collected in the 2θ range 0.06–1.0°, in steps of 0.002° and at a scanning rate of 10 s/point.

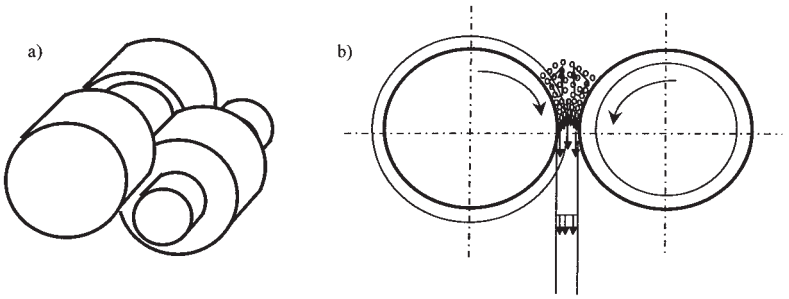

Figure 1 Forming rolls suitable for use in the practice for the formation of a monolithic tape: (a) schematic and (b) side views.

Tensile properties

The tensile properties of the various tapes were examined at room temperature (25°C) with an Instron tensile tester (model 4240, Instron, Canton, MA). The crosshead speed and gauge length were 10 mm/min and 100 mm, respectively. The tensile modulus was calculated with the stress at 0.1% strain. The cross-sectional area of each sample was determined by the measurement of the weight and length of the sample under the assumption that the density of UHMWPE was 1.0 g/cm^3. The maximum draw ratio (λ_{max}) of various compacted tapes was determined at elevated temperatures in the temperature-regulated environmental chamber of the same Instron tensile tester.

Solid-state processing

Solid-state compaction

The compaction device used in the study for the continuous production of the solid-state monolithic tapes from the nascent UHMWPE reactor powders consisted of a pair of the heated rolls that pressed each other (see Fig. 1), with a hollow in one roll and an adequate ledge in the other. Five reactor powders synthesized under different conditions were compacted at the same rolling speed (4 M/min) and temperature (120°C). In addition, the rolling speed and temperature were varied to investigate any morphological changes in the compacted tape. The width of the tape was 20 mm, and the tape was cut into the strips with widths from 1.3 to 5.5 mm before tensile drawing. The tape thickness obtained ranged from 0.1 to 0.2 mm, and the effective draw ratio (λ_{eff}) at rolling, determined from the displacement of an ink mark preimprinted on the strip surface, was about 2–6.

Solid-state drawing

Multistage orientation drawing of the compacted tapes were carried out on the stretching system with heating plates. The temperature at each drawing was gradually increased from 120 to 145°C, which was higher than the melting temperature of the powder yet below the melting point of the oriented tape. The draw ratio at the drawing stage was calculated from the changes in the tape thickness and mass.

Surface analysis

Oxygen plasma treatment

Solid-state-processed UHMWPE filaments were subjected to oxygen plasma treatment in a parallel electrode-type plasma chamber from Vacuum Science (Vacuum Science and Instruments, Daejeon, Korea). The chamber was evacuated to approximately 0.01 Torr and then purged with oxygen gas at a flow rate of 10 sccm. Radio frequency (RF) plasma (13.56 MHz) was used at 50, 100, or 150 W, and the treatment time was 5 min. As soon as the plasma treatment was finished, the fiber samples were subjected to surface characterization or an adhesion study to minimize exposure of the treated fibers to the atmosphere.

Surface characterization

The surface free energy of oxygen-treated UHMWPE filaments was measured by a contact angle analyzer (ERMA contact anglemeter, Goniometer type, model G-1-113-100-0, Tokyo, Japan). The two-liquid probe method with deionized water and methylene iodide (CH_2I_2) was used to separate the polar and dispersive components of the surface free energy, after the procedure of Owens and Wendt.[16] At least 10 fiber samples for each condition were tested, and the average values are reported. In addition, X-ray photoelectron spectrometry (XPS; LVG Scientific, ESCA Lab) was used to investigate the surface chemistry of the oxygen-plasma-treated UHMWPE fibers. The samples were analyzed with Al Kα X-rays at 20 mA and 15 kV, and the pressure was maintained at 1×10^{-9} Torr.

Interfacial adhesion

A carboxyl-terminated butadiene acrylonitrile rubber modified vinylester (Sewon Whasung Co., Seoul, Ko-

TABLE I
Characteristics of UHMWPE Nascent Reactor Powders Synthesized Under Various Polymerization Conditions[14]

Sample code	[Mg] (g/L)	T_{pol} (°C)	P_{C2H4} (psia)	Y (kg of PE/g of Ti hr^{-1} atm^{-1})	M_v ($\times 10^6$)	T_m (°C)	ΔH_f (J/g)
GUR412	—	—	—	—	2.4	141.6	170
10C_15P	4.0	10	15	7	2.7	141.6	208
30C_15P	2.5	30	15	212	1.8	141.5	195
45C_15P	2.5	45	15	230	1.7	141.6	178
60C_15P	2.5	60	15	214	1.0	140.5	184
90C_15P	2.5	90	15	108	0.6	136.6	191
30C_40P	1.25	30	40	250	3.8	143.4	184
90C_40P	1.25	90	40	164	0.5	138.6	192

[Mg] = concentration of magnesium; T_{pol} = polymerization temperature; P_{C2H4} = ethylene pressure; Y = yield; T_m = melting peak point; ΔH_f = enthalpy of fusion.

rea) was used to study the interfacial adhesion of the UHMWPE filaments. The vinylester resin mixed with 1 wt % benzoyl peroxide as an initiator and 13 wt % diallylphthalate as a curing agent was applied to the fiber surface to form a microdroplet approximately 0.4 mm in diameter. After curing at 110°C for 20 min, the size of the microdroplets and embedded fiber length (L) were measured with an optical microscope. Microdroplet tests were conducted on an Instron model 4467 instrument at a crosshead speed of 1 mm/min. The interfacial shear stress (τ) was calculated from the following equation:[17,18]

$$\tau = \frac{F}{\pi D_{eff} L} \quad (1)$$

where F is the pullout force and D_{eff} is the effective diameter of the fiber.

RESULTS AND DISCUSSION

Properties of the UHMWPE powders

The basic properties of the UHMWPE powders synthesized under various reaction conditions are listed in Table I, where the sample code GUR412 denotes a commercial UHMWPE powder (by Ticona, Bayport, TX) and the others denote the newly synthesized UHMWPE powders. The samples were named as in the following example: in 10C_15P, 10C denotes a polymerization temperature of 10°C and 15P denotes an ethylene pressure of 15 psia.

The polymerization of ethylene did not proceed without the addition of a soluble magnesium–organic component of the catalyst system under the reaction conditions studied. The yield of most of the UHMWPE powders ranged from 100 to 250 kg of PE/(g of Ti·h·atm). The yield dropped significantly at temperatures below 20°C and increased with increasing ethylene pressure.

M_v measurements of the UHMWPE powders polymerized under various conditions are depicted in Figure 2. At the same catalyst concentration and ethylene pressure, the molecular weight gradually decreased with increasing polymerization temperature. As a result, the molecular weight went below 10^6 at a high polymerization temperature (90°C).

The UHMWPE reactor powders used in the study exhibited high melting temperatures (137–143°C) and heats of melting (180–210 J/g), as listed in Table I. The high heat of melting of the reactor powders was possibly due to a high ordering of the crystal phase upon polymerization and crystallization at low temperatures.[2,4–8] We can easily surmise that such an untangled conformation became less favorable with increasing polymerization temperature. The melting temperature gradually increased as the polymerization temperature decreased. Each reactor powder exhibited a remarkable difference in melting temperature and heat of melting as determined under two subsequent melting runs, and the difference was more prominent at low polymerization temperatures.

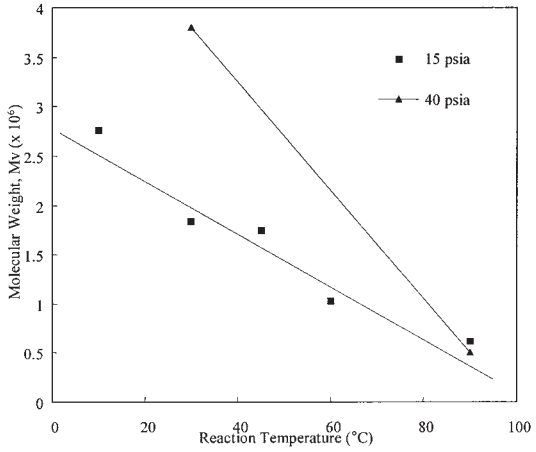

Figure 2 M_v versus the reaction temperature of UHMWPE powders synthesized under various conditions.

TABLE II
Particle Characteristics of UHMWPE Nascent Reactor Powders

Sample code	Bulk density (g/cm^3)	Average particle size (mm)	Average microglobe size (μm)	Micropore volume (cm^3/g)	Micropore inner surface (m^2/g)
GUR412	0.40	0.15	0.9	0.10	1.6
10C_15P	0.10	0.95	0.5	3.09	16.8
30C_15P	0.053	0.50	1.2	2.83	12.5
45C_15P	0.056	0.85	1.0	2.12	17.7
60C_15P	0.055	1.4	0.9	2.31	20.6
90C_15P	0.058	1.0	0.9	2.37	21.1
30C_40P	0.070	1.2	1.3	2.58	30.1
90C_40P	0.058	1.0	1.0	2.36	38.9

Morphologies of the UHMWPE reactor powders

The UHMWPE reactor powders synthesized in this study also had a distinct morphology characterized by a low bulk density (0.05–0.1 g/cm^3), high micropore volume (2–3 cm^3/g), and high micropore inner surface area (10–40 m^2/g), as shown in Table II and Figure 3. The powder morphology of a commercial UHMWPE powder, GUR412, is also shown for comparison. The UHMWPE powders synthesized in this study consisted of anisotropic chip-like particles 0.5–1.5 mm in size. These particles were composed of spherical subparticles 0.5–1.3 μm in diameter, as shown in Figure 3. The surface of the subparticles for the powders polymerized at low temperatures was smooth, whereas it became crinkled with increasing polymerization temperature. There were spacious areas among secondary agglomerates, which represented large micropore volumes of the UHMWPE powder. On the other hand, the commercial UHMWPE powder, GUR412, consisted of much smaller but spherical particles 0.15 μm in size and had narrower particle size distributions than the UHMWPE powders synthesized in this study. There were a significant number of thin fibrils extending from subparticles to others.[19–21] These microfibrils were about 0.1 μm in diameter and occupied most of the spaces among the spherical subparticles. In addition, the GUR412 particles had some evidence of fusion among the exterior layer of subparticles. These differences in the particle morphologies between GUR412 and the UHMWPE powders synthesized in this study resulted in significant differences in the micropore volumes and inner surface areas. Later, we demonstrate that this distinctive particle morphology provided for successful compaction and deformation at temperatures below the melting points of the powders.

Solid-state compaction

Noncontinuous processes

To identify the controlling component in both drawability and tensile properties, various modeling processing experiments on the UHMWPE powder 30C_15P were carried out, and the results are presented in Table III. All the methods listed in Table III were noncontinuous, and the focus of the experiments was on the determination of the controlling component in both the drawability and tensile properties. The powder in a square mold (100 × 100 mm) was pressed at 400 MPa with or without shear deformation. Shearing was performed by repeated pressing of the strip of the pressed sheet at the same conditions. Rolling of the pressed sheet with or without shearing was also carried out for comparison. The pressed sheet of the UHMWPE powder at 30°C could not be drawn at 125°C, whereas the drawing was possible when pressing was done at a higher temperature or when shearing was performed after pressing. Although the shear deformation increased the tensile strength, the rolling after pressing was more effective in enhancing the tensile strength. The modeling experiments in Table III showed that the continuous roll-forming process, composed of simultaneous pressing and rolling, made the tapes suitable for further orientation drawing.

Continuous compaction via roll forming

The continuous production of monolithic UHMWPE tapes was carried out in the roll-forming system, which consisted of a pair of the heated rolls pressed into each other (see Fig. 1). Low-temperature compaction and rolling resulted in a brittle white tape with a density of 0.78–0.9 g/cm^3, which was unable to undergo further orientation drawing. Only roll forming at higher temperatures close to the melting point (110–130°C) resulted in coherent compact tapes. We obtained tapes with thicknesses ranging from 0.1 to 0.2 mm, and λ_{eff} at rolling, determined from the displacement of an ink mark preimprinted on the strip surface, was about 2–6.

In Figure 4, the thermal behaviors of the tapes obtained from the continuous production of various UHMWPE powders are shown. The tapes were processed at the same temperature (120°C), and the roll speed

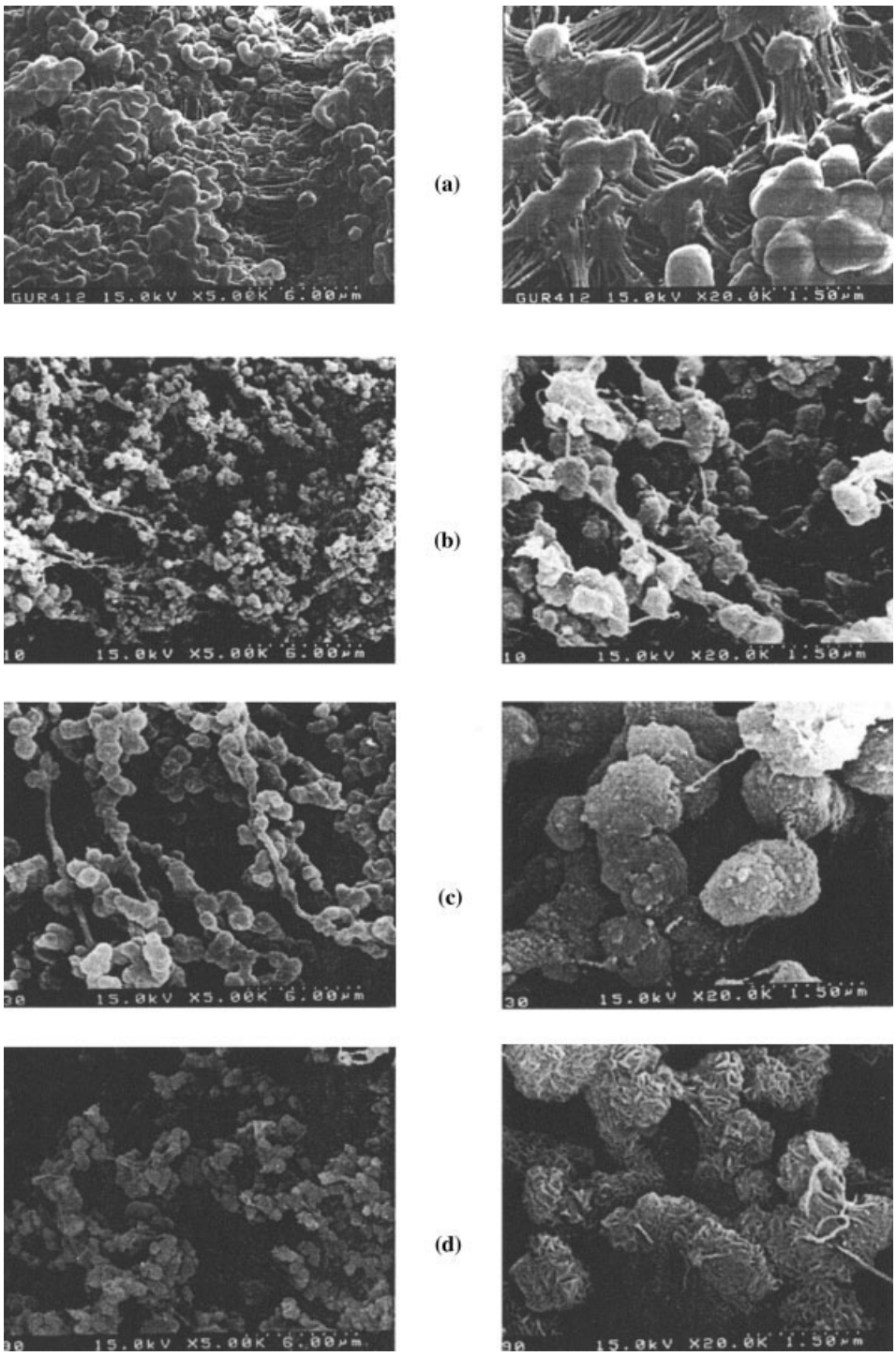

Figure 3 SEM images of various UHMWPE powders: (a) GUR412, (b) 10C_15P, (c) 30C_15P, and (d) 90C_15P.

was kept at 4 M/min. Both the melting temperature and crystallinity increased after solid-state compaction and rolling, and therefore, the tapes made from various UHMWPE powders exhibited even higher melting points (141–144°C) and degrees of crystallinity (70–80%).

The SAXS patterns for the tapes varied substantially depending on the polymerization conditions of the UHMWPE powders used. The long period (L_p) of the tapes determined by the first-order maxima in the SAXS reflections linearly decreased from 40–45 to 27.5–33.5 nm with increasing polymerization temperature (see Fig. 5). The solid-state compaction and rolling of the powders synthesized at higher ethylene pressures resulted in higher values of L_p. The molecular weight dependence on the polymerization tem-

TABLE III
Properties of UHMWPE Tapes Prepared by Various Noncontinuous Processing Methods

Deformation mode	Processing temp. (°C)	λ_{eff}	λ_{max} (at 125°C)	Tensile strength (GPa)
Cold pressing	30	—	—	—
Cold pressing and shearing	30	2.0	24	0.8–0.9
Cold pressing and rolling	30	5.6	24	1.8–1.9
Cold pressing, shearing, and rolling	30	3.4	22	1.7–2.0
Hot pressing	120	—	45	0.9–1.1
Hot pressing and rolling	120	3.9	20	1.3–1.7

perature and ethylene pressure coincided with the trends for L_p described previously. The lamellar thickness [fold length (L_f)] values of the tapes, calculated from L_p and crystallinity, are also shown in Figure 5(b). Because of their higher degrees of crystallinity, the L_f values of the tapes from the UHMWPE powders synthesized at low ethylene pressures were slightly higher than those of tapes from high-ethylene-pressure UHMWPE. The SAXS reflection intensity decreased with increasing polymerization temperature and ethylene pressure. Any first-order maxima in the SAXS reflection were not observed in simple pressed sheets or in the tapes processed at temperatures below 100°C. Hence, the preparation of well-stacked lamella during roll forming was very important for the subsequent successful drawing of UHMWPE tapes below their melting temperatures.

The formation of layered lamella during roll forming of the UHMWPE powders was also observed in the SEM images of the tapes, as shown in Figure 6. The processed tapes were etched with a $7K_2CrO_7$: $150H_2SO_4$:$12H_2O$ solution for 1 h before the SEM study. In Figure 6, the white areas correspond to the crystallites, which were layer-like and separated by amorphous regions (the dark parts) because of selective removal by the etching solution. The L_f values obtained in this SEM study of the etched tapes were in good agreement with those from the SAXS study.

Solid-state orientation drawing

λ_{max}

Before the continuous solid-state multistage orientation drawing experiments, the drawability of the tapes made from various UHMWPE powders was investigated via the determination of λ_{max} at several drawing temperatures still below the melting point in the Instron tensile tester. For stacked lamellar crystals, λ_{max} was estimated by the ratio of L_f and the chain diameter (δ):[2]

$$\lambda_{max} = L_f/\delta \quad (2)$$

In contrast to the theoretical estimate given by eq. (2), we observed that the drawability sensitively depended on both the polymerization and drawing conditions. In Figures 7 and 8, the λ_{max} values of tapes at two different strain rates (10 and 50 cm/min) are plotted against the polymerization and drawing temperatures, respectively. The strain rate of 50 cm/min was the highest value in the Instron tensile tester, and the typical strain rate in the continuous solid-state multistage orientation drawing experiments was much higher (4–15 M/min). λ_{max} steadily increased with increasing polymerization and drawing temperatures at a high strain rate (50 cm/min), whereas λ_{max} at a relatively lower strain rate (10 cm/min) changes

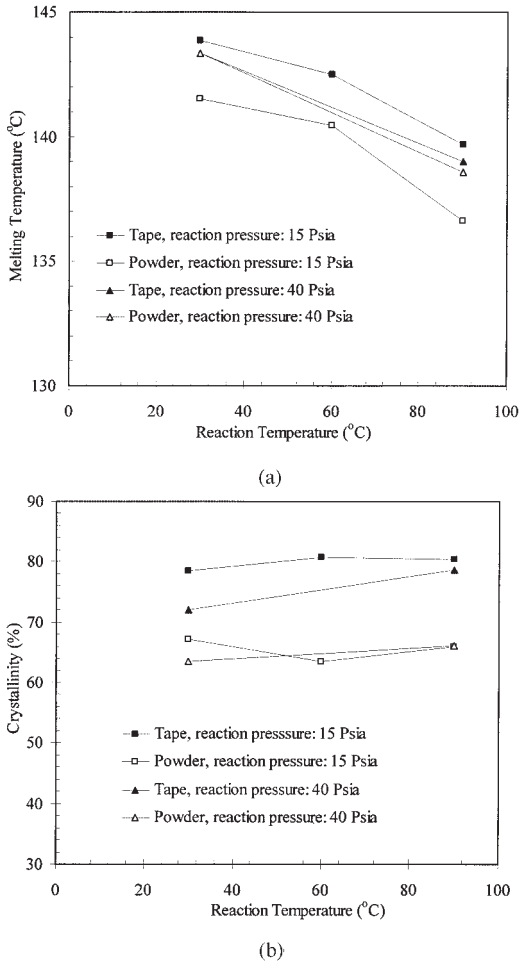

Figure 4 Thermal behaviors of compacted UHMWPE tapes at temperatures below their melting points. Various UHMWPE powders polymerized under different conditions were used: (a) melting temperature and (b) heat of fusion versus the reaction temperature.

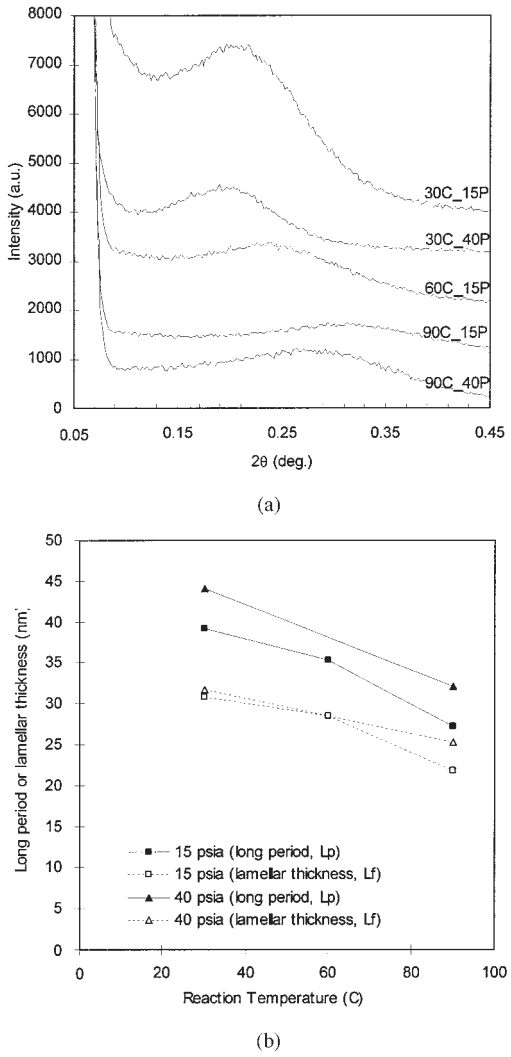

Figure 5 SAXS analysis of UHMWPE tapes compacted with various UHMWPE powders: (a) SAXS patterns and (b) L_p and L_f versus the polymerization temperature.

with the polymerization and drawing temperatures in a complex manner; for the tapes made from low-temperature UHMWPE, λ_{max} steadily increased with increasing drawing temperature, whereas λ_{max} decreased at high drawing temperatures for powders synthesized at 90°C. As a result, at high drawing temperatures (125 and 130°C), λ_{max} for 30C_15P was higher than for 60C_15P and 90C_15P. This tendency of decreasing λ_{max} with reaction temperature at low deformation rates and high drawing temperatures coincided with the theoretical estimate given by eq. (2) and based on L_f. Finally, the UHMWPE powder synthesized at a low temperature and high ethylene pressure, 30C_40, resulted in the lowest λ_{max} at all of the drawing temperatures examined. Despite its relatively large L_f, the high molecular weight of the polymer synthesized at a high pressure appeared to restrict opportunities for chain extension and, thus, uniaxial drawing, despite its successful compaction into a coherent tape.

Multistage drawing orientation

The multistage orientation drawing of the compacted tapes was carried out on the stretching system with heating plates.[15] The temperature at each drawing was gradually increased from 120 to 145°C. The total draw ratio (λ) of the drawn samples was calculated by the multiplication of λ_{eff} in the tape compaction by the draw ratio achieved in the multistage orientation drawing. At relatively low λ's (<30), the tensile strength increased with decreasing width of the strip cut. This may imply that nonuniform orientation across the tape resulted in a reduction in the tensile properties, and only tapes with narrow widths provided opportunities for uniform chain extension throughout the entire uniaxial drawing of the compacted tapes. However, a narrow width of the strip

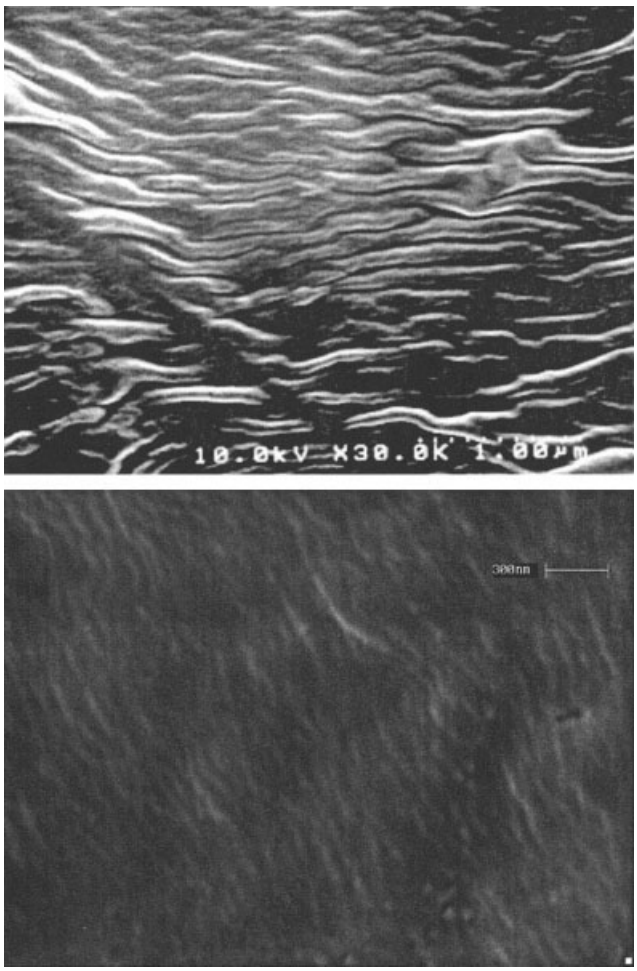

Figure 6 SEM images of UHMWPE tapes made from (a) 30C_15P and (b) 90C_40P UHMWPE powders. The tapes were etched with a $7K_2CrO_7$:$150H_2SO_4$:$12H_2O$ solution for 1 h.

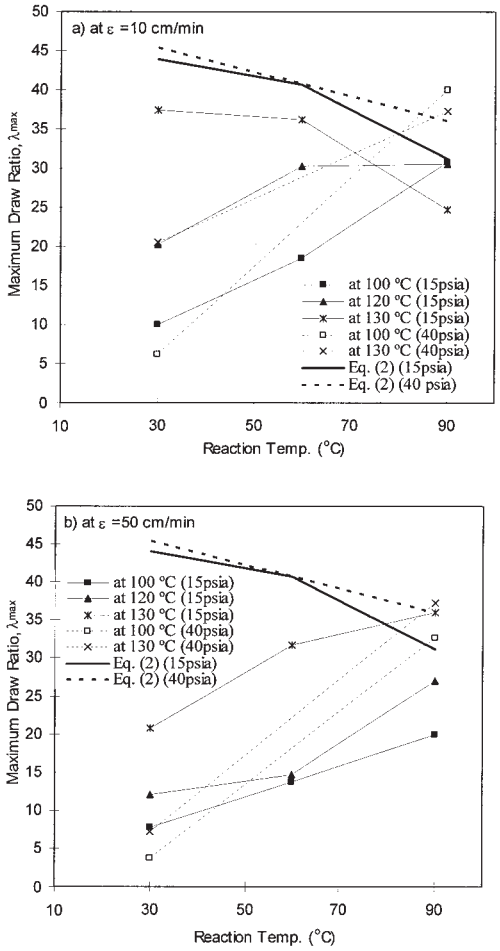

Figure 7 λ_{max} versus the polymerization temperature of UHMWPE compacted tapes at various drawing temperatures. Data at two different drawing rates are shown: (a) 10 and (b) 50 cm/min. Theoretical estimates of λ_{max} are also shown in the plot.

(<1.3 mm) caused frequent cutting of the tape at higher λ's (>45) in the multistage drawing experiments. As a result, the fiber drawn to λ = 90 in the multistage drawing experiments with a strip width of 3.8 mm had a tensile strength of 2.5 GPa and a tensile modulus of 130 GPa. The following results from the multistage drawing experiments were obtained with a wide-width strip (5.5 mm) to prevent frequent cutoff during the multistage drawing orientation.

In Figure 9, the effects of the polymerization conditions of the UHMWPE powders on the tensile properties of the drawn filaments at the same drawing conditions are shown. Both the tensile strength and modulus gradually increased with increasing draw ratio. For the low-temperature powders 30C_15P and 30C_40P, the increase in the tensile strength was reduced at λ values higher than 20, whereas tapes from powders synthesized at 90°C showed a steady increase in the tensile strength. The tensile modulus increased with decreasing polymerization temperature, whereas the drawing of low-temperature UHMWPE powders resulted in lower tensile strengths.

The tensile properties of the tapes obtained at four different drawing conditions are illustrated in Figure 10. In this multistage drawing experiment, two different drawing rates (4 and 8 M/min) at each stage were applied at two different drawing temperature gradients (120–130 and 120–140°C). Drawing the tape at the relatively low drawing rate (4 M/min) and higher temperature gradient [120–140°C; Low Deformation at High Temperature (LDHT) in Fig. 10] resulted in the highest tensile properties, whereas drawing at the high rate (8 M/min) and low temperature gradient [120–130°C; High Deformation at Low Temperature (HDLT)] yielded the lowest values in tensile properties at the same λ. The tensile properties did not sensitively depend on the drawing rate if a relatively low temperature gradient was applied. From these results, we conclude that drawing at a relatively low rate and a high temperature gradient was essential in the continuous production of high-strength, high-modulus UHMWPE fibers at temperatures below the melting point.

The peak melting temperature of drawn UHMWPE filaments made from the UHMWPE powder 30C_15P

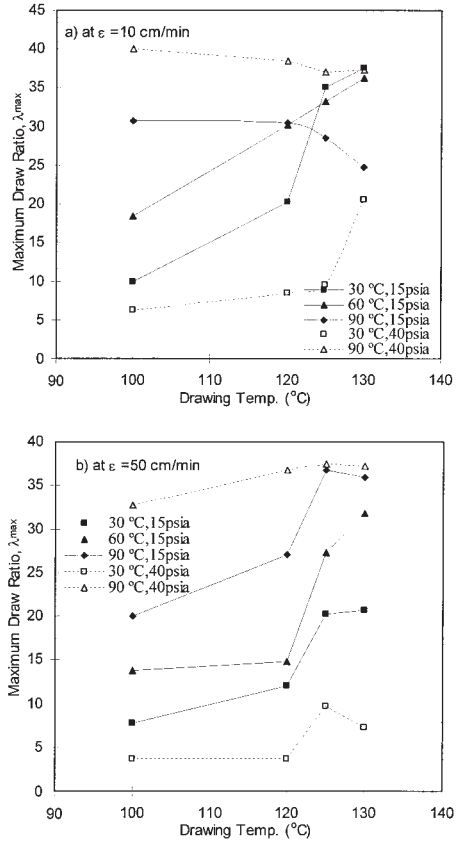

Figure 8 λ_{max} versus the drawing temperature of UHMWPE compacted tapes. Data at two different drawing rates are shown: (a) 10 and (b) 50 cm/min.

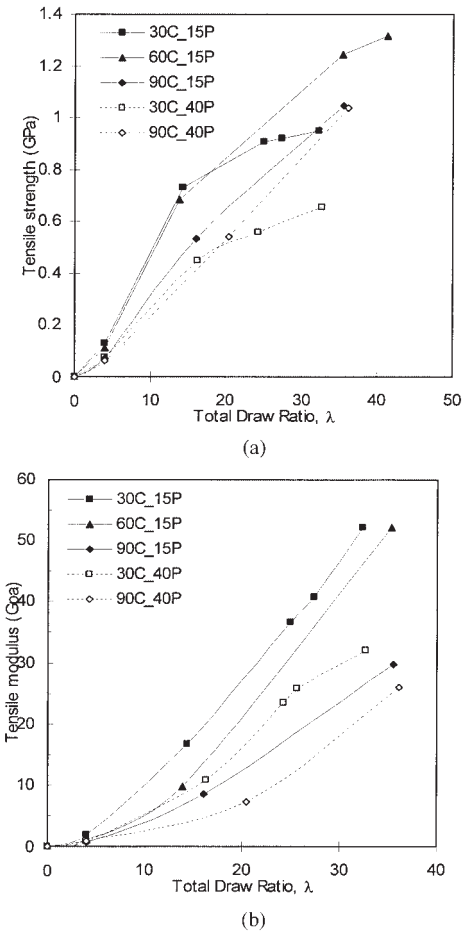

Figure 9 Effects of the polymerization conditions on the tensile properties of drawn UHMWPE filaments: (a) tensile strength and (b) tensile modulus versus λ.

at two different drawing rates are depicted in Figure 11. The melting temperature gradually increased with increasing λ at both drawing rates, and drawn tapes started to exhibit double endothermic peaks at high draw ratios. The relative sizes and peak temperatures of these two peaks heavily depended on the drawing rate. The second endothermic peak at a higher temperature disappeared after rapid cooling and subsequent reheating (the second melting run). Therefore, the appearance of the double peaks at higher temperatures must have been caused by highly aligned crystallite structures in the filament. The formation of highly aligned crystallite structures during the multistage, solid-state drawing process are also be discussed with the results of the SAXS study of the filaments. The appearance of the double peaks has been observed in the thermal analysis of gel-spun UHMWPE fibers,[22] whereas the sharp single endothermic peak has typically been observed in many conventional solid-state drawings of UHMWPE reactor powders.[8,9,23]

The changes with increasing draw ratio in the SAXS patterns of the UHMWPE filaments made from the UHMWPE powder 30C_15P are illustrated in Figure 12. The first-order maxima in the SAXS reflections linearly decreased with increasing draw ratio and eventually disappeared at high draw ratios. Therefore, L_p of the tapes determined by the first-order maxima linearly increased, and a chain-extended conformation of the UHMWPE molecules seemed to be obtained. The SAXS reflection intensity also decreased with increasing draw ratio. Clements and Ward[24] explained the observed decrease in SAXS reflection intensity at higher draw ratios by an increase in the formation of crystalline bridges acting as link between oriented lamellae, whereas Peterlin and Corneliussen[25] ascribed it to a decrease in the effective electron density difference between the amorphous and crystalline components. L_p values determined by the first-order maxima of the SAXS reflections in this study (45–60 nm) were rather higher than those from gel-spun fibers[22] or previous solid-state drawing experiments in literature.[26–30] In a later communication, the structural analysis, including the deformation mechanism on the solid-state drawing of the UHMWPE powders used in this study, will be thoroughly presented.

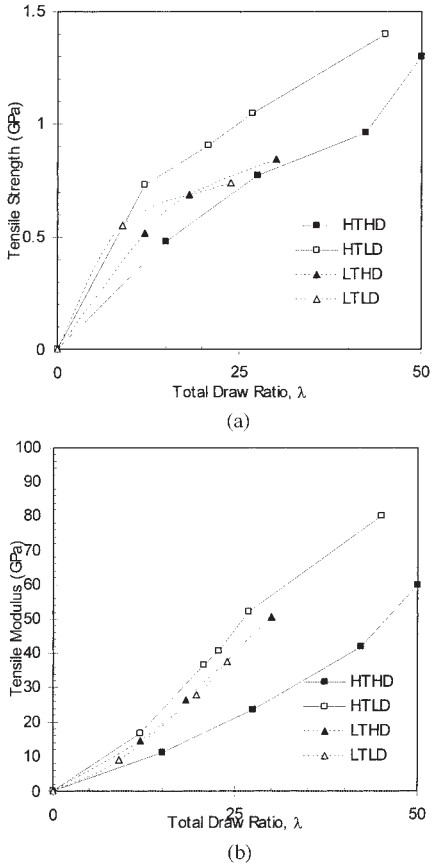

Figure 10 Effects of the drawing temperature and rate on the tensile properties of drawn UHMWPE filaments made from the UHMWPE powder 30C_15P: (a) tensile strength and (b) tensile modulus versus λ.

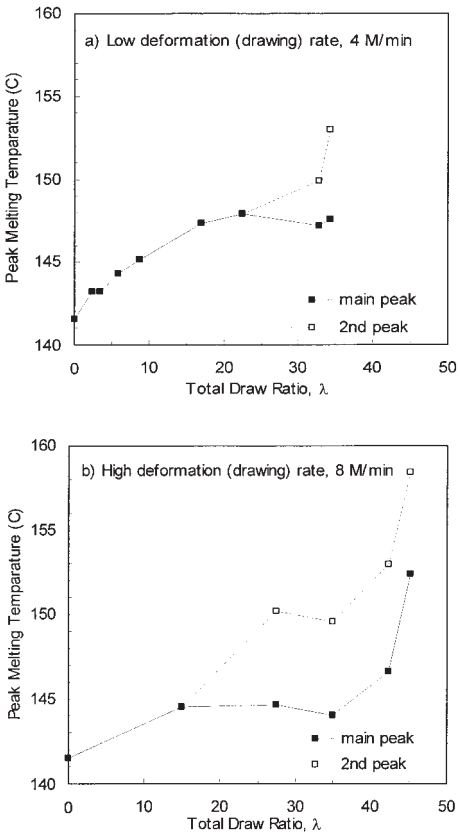

Figure 11 Thermal behaviors of drawn UHMWPE filaments made from the UHMWPE powder 30C_15P. The peak melting temperature for two different drawing routes are plotted versus λ: (a) low deformation rate (4 M/min) and (b) high deformation rate (8 M/min).

Surface modification of solid-state drawn filaments

Surface analysis

To improve the adhesion of solid-state processed UHMWPE filaments to a matrix, the filaments were treated with oxygen plasma under various conditions. To determine the changes in the surface free energy of the filaments, the contact angle on water and methylene iodide were measured. The obtained surface free energy was divided into polar and nonpolar components and are listed in Table IV. As seen in the table, the surface energy was substantially increased by oxygen plasma treatment. The increase in the surface energy was mostly from that of the polar components. To identify the polar components, the XPS study was carried out for the UHMWPE fibers with and without plasma treatment, and the C1s peaks of both samples are compared in Figure 13. Peak deconvolution indicated four possible peaks in the plasma-treated sample: C—H (285.0 eV), C—O (286.7 eV), C═O (2881. eV), and O═C—O (289.4 eV), whereas the contribution of these oxygen-containing moieties was virtually absent in the untreated sample. Hence, both the contact angle measurements and XPS analysis indicated that the formation of polar groups, such as ketone, carboxyl, and hydroxyl groups, on the surface of the fiber by oxygen plasma treatment increased the affinity with water, as shown by the decrease in the contact angle with water.

Interfacial shear strength

As expected from the increased surface free energy and polar components, the interfacial shear strength of the UHMWPE fibers, evaluated via microdroplet tests, increased with plasma treatment. The interfacial shear strength of the UHMWPE fibers with the vinylester resin with increasing plasma power is shown in Figure 14. The shear strength reached its maximum at about 100 W. The slight decrease in the shear strength at 150 W was possibly due to the degradation of fibers from the high plasma power.

Finally, the deformation behavior of the surface-treated UHMWPE fibers during the microdroplet tests are compared with that of the untreated sample in Figure 15. For the untreated sample, debonding took places at a very small displacement and a low loading because of poor interfacial adhesion between the fiber and matrix, whereas the interfacial shear force increased significantly for the plasma-treated fibers. This result indicates that increased surface free energy and polar components by oxygen plasma treatment, in turn, enhanced the impregnation of the matrix and chemical bonding at the fiber surface.

CONCLUSIONS

In this article, we presented observations on continuous solid-state processing of UHMWPE nascent reactor powders into highly drawn tapes. First, a UHMWPE reactor powder with a high yield even at low

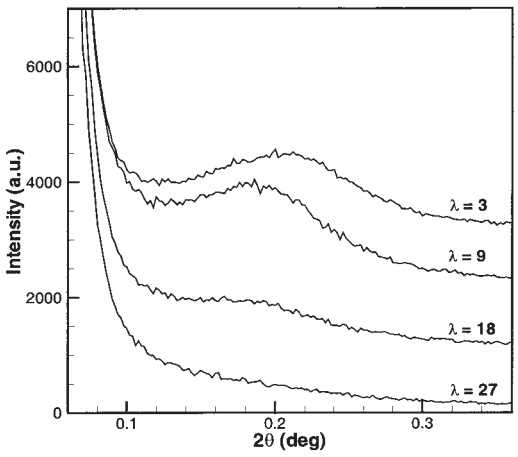

Figure 12 Changes in the SAXS patterns of UHMWPE filaments made from the UHMWPE powder 30C_15P with increasing draw ratio.

TABLE IV
Results of the Contact-Angle Analysis of Solid-State Processed UHMWPE Tape Filaments with Oxygen Plasma Treatment Conditions

Plasma treatment condition	Contact angle (°)		Nonpolar component (ergs/cm^2)	Polar component (ergs/cm^2)	Total surface free energy (ergs/cm^2)
	Water	Methylene iodide			
Untreated	94.8	64.4	26.73	1.66	28.39
50 W, 5 min	15.0	60.0	29.33	41.98	71.32
100 W, 5 min	9.8	51.6	34.25	39.60	73.85
150 W, 5 min	3.0	45.2	37.87	37.99	75.86

reaction temperatures was prepared by the polymerization of ethylene in the presence of soluble magnesium complexes. We demonstrated that the soluble magnesium complex catalyst system provided a unique, microporous powder morphology, which resulted in the successful compaction of UHMWPE powders into coherent tapes at low temperatures. The SAXS study of the compacted tapes revealed that folded-chain crystals with a relatively long range order were formed during the compaction and were transformed extended-chain crystals.

We also investigated the effects of the reaction conditions and key parameters of the solid-state processing on the tensile and thermal properties of the coherent UHMWPE tapes by direct roll forming at temperatures below their melting points and by a subsequent multistage orientation drawing at elevated temperatures below the melting point of the tape. The cut width of the tapes, the deformation rate, and the temperature were varied in the drawing process, and the thermal behavior and tensile properties of the drawn tapes were measured with increasing draw ratio. The thermal behavior and tensile properties of the drawn tapes depended sensitively on the polymerization conditions and on key parameters in the solid-state processing. The fiber drawn to $\lambda = 90$ in the study had a tensile strength of 2.5 GPa and a tensile modulus of 130 GPa. Finally, the enhancement of the interfacial shear strengths of the solid-state drawn UHMWPE filaments with vinylester matrix by O_2 plasma treatment was presented.

The drawing characteristics and tensile properties of the highly drawn UHMWPE fibers are not discussed in this article. Only the UHMWPE powders, which met strict requirements for thermodynamic and morphological characteristics, could be drawn up to a λ higher than 100 without frequent cutting of the filament. Further experimental studies of the drawing characteristics and properties of highly drawn UHM-

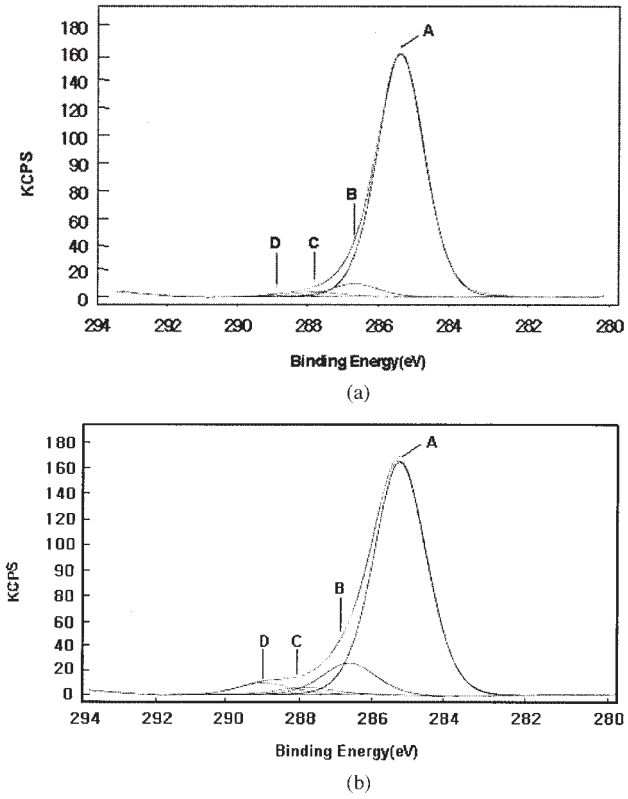

Figure 13 Deconvoluted peaks [(A) —C—H, (B) —C—OH, (C) ═C═O, and (D) —COOH] from the XPS results of the UHMWPE filaments: (a) untreated and (b) O_2-plasma-treated (100 W, 5 min) filaments. KCPS = kilo counts per second.

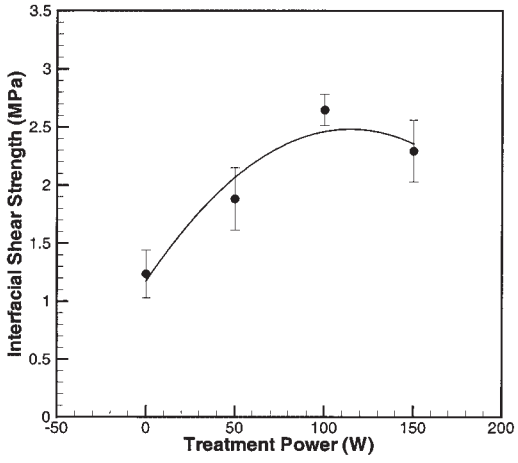

Figure 14 Effect of the treatment power on the interfacial shear strength of the UHMWPE filaments.

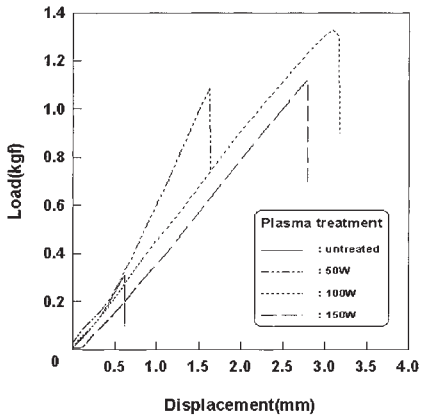

Figure 15 Load versus displacement curves of UHMWPE fibers from the pullout test with various O_2 plasma treatments.

WPE fibers with higher strengths and moduli are underway.

The authors thank Jung Yoon Do for preparing the organic magnesium complexes used in the study. Furthermore, they gratefully acknowledge Tae Yoong Yeo for performing the X-ray diffraction measurements.

References

1. Porter, R. S.; Chuah, R. S.; Kanamoto, T. In High Modulus Polymers; Zachariades, A. E.; Porter, R. S., Ed.; Marcel Dekker: New York, 1988; p 259.
2. Lemstra, P. J.; Bastiaansen, C. W. M.; Rastogi, S. In Structure Formation in Polymeric Fibers; Salem, D. R., Ed.; Hanser Gardner: Cincinnati, OH, 2001.
3. Zachariades, A. E.; Kanamoto, T.; Porter, R. S. In Polymer Powder Technology; Narkis, M.; Rosenzweig, N., Ed.; Wiley: New York, 1995; p 427.
4. Chanzy, H.; Day, A.; Marchessault, R. H. Polymer 1967, 8, 567.
5. Smith, P.; Chanzy, H. D.; Rotzinger, B. P. Polym Commun 1985, 26, 258.
6. Smith, P.; Chanzy, H. D.; Rotzinger, B. P. J Mater Sci 1987, 22, 523.
7. Rotzinger, B. P.; Chanzy, H. D.; Smith, P. Polymer 1989, 30, 1814.
8. Wang, L. H.; Ottani, S.; Porter, R. S. Polymer 1991, 32, 1776.
9. Seliknova, V. I.; Zubov, Y. A.; Sinevich, E. A.; Chvalun, S. N.; Ivancheva, N. I.; Smol'yanova, O. V.; Ivanchev, S. S.; Bakeev, N. F. Polym Sci USSR 1992, 34, 151.
10. Kanamoto, T.; Ohama, T.; Tanaka, K.; Takeda, M.; Porter, R. S. Polymer 1987, 28, 1517.
11. Otsu, O.; Yoshida, S.; Kanamoto, T.; Porter, R. S. Proceedings of the Polymer Processing Society; Japan Society of Polymer Processing: Tokyo, Japan, 1988.
12. Akira, S.; Hirofumi, K.; Yoshimu, I.; Shigeki, Y.; Kazuo, M. Eur. Pat. EP0376423 (1990).
13. Won, H. Y.; Song, J. K.; Joo, Y. L.; Lee, H. K.; Park, N. C. Korean Pat. KP00–274792 (2000).
14. Joo, Y. L.; Han, O. H.; Lee, H. K.; Song, J. K. Polymer 2000, 41, 1355.
15. Won, H. Y.; Song, J. K.; Joo, Y. L.; Lee, H. K.; Park, N. C. Korean Pat. KP00–274657 (2000).
16. Owens, D. K.; Wendt, R. C. J Appl Polym Sci 1969, 13, 1741.
17. Lee, S. G.; Kang, T. J.; Yoon, T. H. J Adhes Sci Tech 1998, 12, 731.
18. Li, Z.-F.; Netravali, A. N.; Saches, W. J. Mater Sci 1992, 44, 4625.
19. Halldin, G. W.; Mehta, S. D. Soc Plast Eng Annu Tech Conf 1983, 29, 238.
20. Truss, R. W.; Han, K. S.; Wallace, J. F.; Geil, P. H. Polym Sci Eng 1980, 20, 747.
21. Barnetson, A.; Hornsby, P. R. J Mater Sci Lett 1995, 14, 80.
22. Fu, Y.; Chen, W.; Pyda, M.; Londono, D.; Annis, B.; Boller, A.; Habenschuss, A.; Cheng, J.; Wunderlich, B. J Macromol Sci Phys 1996, 35, 37.
23. Wang, L. H.; Porter, R. S. J Appl Polym Sci 1991, 43, 1559.
24. Clements, J.; Ward, I. M. Polymer 1983, 24, 27.
25. Peterlin, A.; Corneliussen, R. Makromol Chem A-2 1968, 6, 1273.
26. Furuhata, K.; Yokokawa, T.; Seoul, C.; Miyasaka, K. J. Polym Sci Polym Phys Ed 1986, 24, 59.
27. Kanamoto, T.; Tsuruta, A.; Tanaka, K.; Takeda, M.; Porter, R. S. Macromol 1988, 21, 470.
28. Chvalun, S. N.; Poshastenkova, A. B.; Bakeev, N. F. Polym Sci USSR 1992, 34, 161.
29. Ogita, T.; Kawahara, Y.; Nakamura, R.; Ochi, T.; Minagawa, M.; Matsuo, M. Macromolecules 1993, 26, 4646.
30. Butler, M. F.; Donald, A. M.; Ryan, A. J. Polymer 1998, 39, 39.